

## **A new downhole geophysical observatory for near-field monitoring and real-time subsurface management.**

**Philippe A. Pezard<sup>1</sup>, Hervé Perroud<sup>1</sup>, Johana Lofi<sup>1</sup>, Stéphanie Gautier<sup>1</sup>,  
Gilles Henry<sup>1</sup>, Muriel Geeraert<sup>1</sup>, Agathe Deleau<sup>1</sup>,  
Géosciences Montpellier, UMR 5243 CNRS-UM2, Montpellier, France,  
Denis Neyens<sup>2</sup>, Simon Barry<sup>2</sup>,  
imaGeau, Cap Oméga, Montpellier, France,  
Arnaud Levannier<sup>3</sup>,  
Schlumberger Water Services, Den Haag, The Netherlands.**

Initially as part of the European Community (EC) funded ALIANCE project (FP5), a new kind of near-field, high frequency downhole hydrogeophysical observatory was designed, constructed and set-up at two different Mediterranean field sites in terms of geological context, hydrological regime and local human impact. This new downhole approach was first deployed near Montpellier (France) at the Maguelone experimental site and conceived for long-term *in-situ* monitoring and prevention of brine intrusion in coastal aquifers.

The principle of the observatory is based on the high-frequency (such as daily) probing of the formation electrical resistivity around a borehole over periods of several years. For so-called “real-time” subsurface management, this device is aimed at producing accurate near-field boundary conditions to reduce uncertainties in models, and thereby contribute to the decision-making process for endangered aquifer management.

At present, the system is being applied to groundwater management, risk management in the context of salt-water intrusion in coastal aquifers, or else the depollution of petrochemical industrial sites. A new double cask version for deep deployment in the context of CO<sub>2</sub> geological sequestration has been constructed and deployed lately at Maguelone for testing in the context of the FP7 EC MUSTANG project.

Keywords: hydrogeophysics, electrical properties, downhole monitoring, salt water intrusion.

## **Introduction**

Over 50 % of the accessible water at or near the Earth surface is over-exploited due to human activities. Groundwater is particularly at risk in urban or semi-arid areas, with the maximum danger in coastal zones where more than 60% of the world population is concentrated. As the main source of drinking water, this strategic but vulnerable resource is of utmost importance.

Salt intrusion in coastal aquifers, either from natural or anthropogenic source, is often related to over-drafting due to agricultural use, a high density of population, or the effect of droughts in arid regions. While the physical processes associated with salt-water intrusion are still being discussed, more field data are needed to assess the predictive models developed for long-term management and vulnerability assessment of groundwater resources in coastal environments. For this, the ALIANCE research project focused on the development of new hydrogeophysical logging sensors and long-term monitoring methods to describe and monitor saline intrusion processes. The overall objective was to improve groundwater sustainability and quality in coastal and semi-arid environments.

For this, the aim of ALIANCE was to develop, integrate and assess a set of new geophysical tools, methods and scientific approaches to obtain an improved description of aquifer and fluid parameters in the subsurface. In particular, a new permanent downhole method was conceived for long-term *in-situ* monitoring and prevention of brine intrusion in coastal aquifers. The principle of the observatory is based on the high-frequency (such as daily) probing of the aquifer electrical resistivity around a borehole over periods of several years.

In particular, the slow renewal of groundwater, especially in semi-arid regions, enhances the need for long-term management tools. In order to mitigate the risks of long-lasting pollution or over-abstraction in such exposed aquifers, it is necessary to improve exploration and monitoring methods for the subsurface, to describe with an improved precision aquifer characteristics and fluid flow dynamics. Such improvements are also needed to develop, test and validate new theoretical and numerical models which are, in turn, necessary to assess and plan ahead aquifer vulnerability or groundwater sustainability and quality. The development of integrated approaches is requested to link exploration, monitoring, modelling and management facilities.

Finally, the cornerstone of the ALIANCE project was the setting-up of field in-situ facilities for experimentation and long-term monitoring. The European community includes a large number of potentially exposed coastal aquifers due to over-exploiting and/or natural drought, especially in the Mediterranean region. At Maguelone located 10 km south of Montpellier (France) along the mediterranean shoreline, one of the three new ALIANCE coastal experimental sites was developed purely for instrumental purposes.

### **Maguelone experimental site and geological context**

The Maguelone experimental site is located along the Mediterranean lido of the Gulf of Lions passive margin, 10 km to the south of Montpellier. Limited to the north by the Prevost coastal lagoon and to the south by the Mediterranean Sea (*Figure 1*), this site offers a natural laboratory to study porous coastal reservoirs in a clastic and clay-rich context saturated mostly with saline fluids.

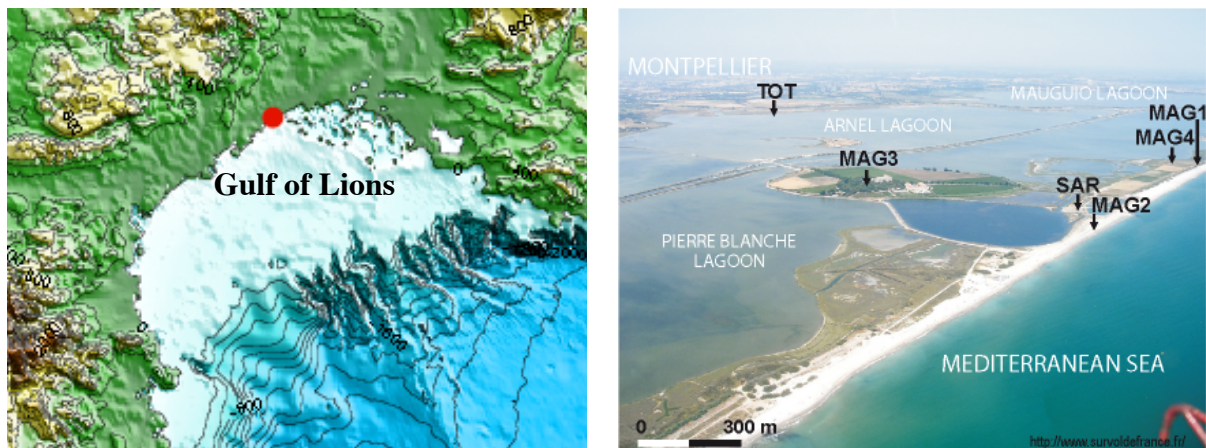


**Figure 1.** Geographical location (left) and aerial photograph (right) of the Maguelone experimental site located to the NW of the photograph (with the MAG1 and MAG4 boreholes) and one km to the east of the Maguelone island (with the MAG3 borehole).

Five shallow boreholes (12 to 60 m deep) were drilled from 2003 to 2004 at Maguelone over 5 km<sup>2</sup> for geological, hydrological and instrumental reasons in the framework of EC “ALIANCE” project (Figure 1). This project was dealing with the development and field testing of new geophysical methods and instruments to document salt-water intrusion in porous coastal aquifers. For this, one of the boreholes (MAG4) was dedicated to the deployment of the first downhole and high resolution observatory of electrical resistivity. This new observatory provides daily and m-scale downhole resistivity profiles to follow the changes over time of pore fluid salinity in the formations penetrated by the hole. At this site, continuous geological samples (from MAG1) and geophysical data from shallow boreholes outline the presence of two distinct depositional sequences :

- Near the ground surface (0-9 m), a thin Late-Holocene sequence (< 5000 yrs B.P.) is constituted with lagoon sediments with impermeable dark green clays topped by grey shelly beach sands. This sequence forms an impermeable seal overlying the Pliocene sequence with an unconformity.
- A Pliocene sequence, from 9 m depth to the base of MAG1 ((0 m). This sequence consists mainly in relatively homogeneous fine grained continental deposits (clays, silts, and clayey silts). Locally, some marine incursions (grey clays) and lacustrine levels (white carbonates clays) are visible. The clayey fraction is relatively high all along the sequence, making those deposits relatively poorly permeable.

In this sequence, a single remarkable depositional unit is located from about 13 to 16 m depth and consists in a porous and permeable conglomerates and sands interpreted as fluvial deposits. The conglomerates, clearly identified downhole from low natural gamma radioactivity values, can be correlated laterally with boreholes located at a km distance, showing the lateral extension of this unit. Sedimentary facies and geophysical measurements suggest a high permeability and porosity for these conglomerates, also bounded above and below by clay-rich horizons. Also, hydrogen sulphite (H<sub>2</sub>S) was encountered during drilling operations when the drill went through this horizon. The possibility of the conglomerate



- **Downhole Seismic Observatory (MAG1):** the first hole drilled and fully cored in 2003 to a depth of 60 m was equipped with a PVC liner down to 59 m, and with a slotted PVC liner from 59 to 63 m. However, the bottom 4 meters of the hole were found to be obstructed by fine grain sediments only a few hours after drilling, yielding a total depth of 59 m which has remained unchanged since drilling. Open at the base and artesian for a few tens of minutes from about 40 m depth, the hole has been producing water from its base since initial drilling, and with an electrical resistivity of  $8.0 \Omega \cdot \text{m}$  (or  $1250 \mu\text{S}/\text{cm}$  of fluid conductivity, equating to a pore fluid salinity of about one g/L). In the new MUSTANG spread, MAG1 is now used to install a downhole seismic observatory in order to complete the overall geophysical strategy and study how different methods might be combined for a more efficient description of the saturation/desaturation process associated with gas injection in the conglomerate.
- **Downhole Electrical Observatory (MAG4):** the first resistivity observatory prototype was constructed and set-up in June 2004 in a borehole (MAG4) located 50 m to the NW of MAG1. The observatory was equipped from surface to 41 m depth with permanent electrodes with a spacing of one meter. It was tested in Wenner, dipole-pole and dipole-dipole modes, and calibrated against induction resistivity logs recorded in MAG1. A good coherency between dipole-dipole data and medium induction resistivity (*Figure 3*) was found, both probing the electrical resistivity of the formation at meter scale. For example, both electrical methods measure a local increase in electrical resistivity found to coincide in space with low gamma values from the conglomerate reservoir and corresponds to pore space desaturation associated with the presence of gas. Time-lapse resistivity measurements were made automatic from 28 to 40 m in 2006 (*Figure 4*), showing very gradual but continuous changes over time in electrical resistivity at the base of the hole.

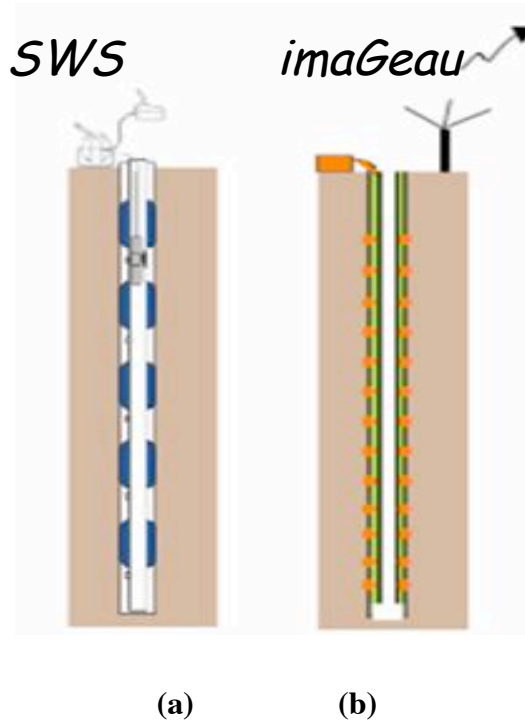


**Figure 3.** Permanent & downhole instrumentation ; (a) downhole hydrochemical observatory based on a WestBay multipacker completion (provided by Schlumberger); (c) downhole electrical observatory (provided by imaGeau).

- Downhole Hydrochemical Observatory (MAG5):** this downhole hydrochemical observatory (*Figure 4*) is based on a multi-packer completion from WestBay (Schlumberger), including packers in order to provide fluid samples, temperature and pressure records during injection and thereby time/space calibration points from tracers (i.e. precise boundary conditions) to numerical modelers. Eight zones were equipped for fluid sampling and monitoring down to a depth of 49 m. For experimental purpose as part of MUSTANG, two of these zones were located within the reservoir (at 13.9 and 15.5 m), one above (at 7.9 m) and a fourth one below (24.9 m). For long-term survey of underlying groundwater, another set of four sampling zones was installed in front of sand-rich layers (*Figure 3*) to allow probing at 32.1, 36.7, 39.8 and 49.0 m.

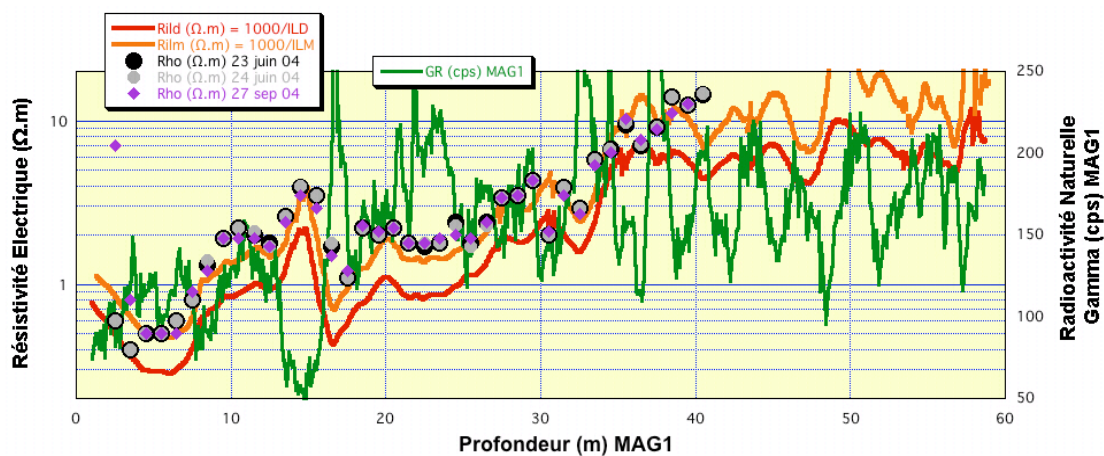


**Figure 4.** Calibration of electrical resistivity data recorded in 2003 in MAG4 in a dipole-dipole mode from induction resistivity logs recorded through PVC liner in MAG1. Downhole observatory data are presented with black (June 23, 2004), grey (June 24, 2004) and purple dots (September 27, 2004), while medium (orange) and deep (red) induction logs appear as continuous traces. The downhole gamma radioactivity profile (green curve) provides a lithological reference to underline the presence of clays, and the conglomeratic reservoir at 13 to 16 m depth.

Excellent repeatability over time is shown for the entire observatory by measurements recorded during successive days in June. The profile recorded in September is also very similar to the previous ones in front of clay-rich horizons, with departures in the conglomeratic layer, some sand-rich layers, and close to surface due to desaturation from surface during summer.

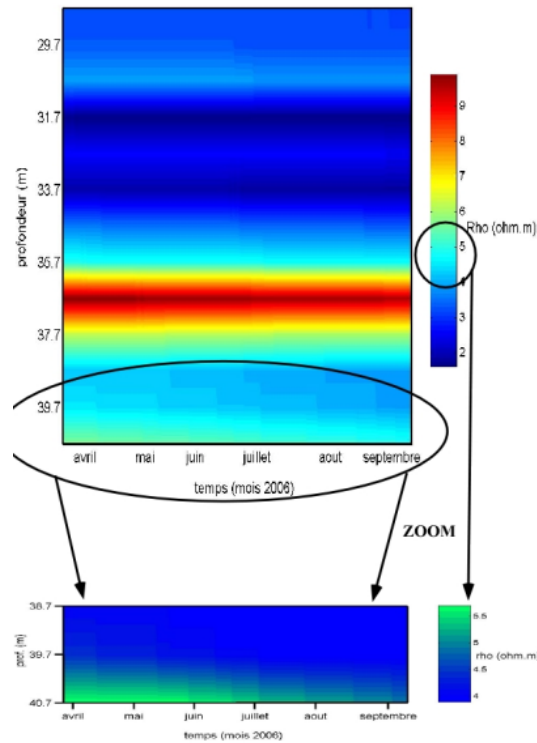


**Figure 5.** Downhole electrical resistivity data recorded daily with the CNRS-ALIANCE prototype over a 6 months period (April to September 2006) from 29 to 40 m depth.

This electrical resistivity map (Figure 5) demonstrates the stability of the measurement device over time. At the base of this interval, a gradual resistivity decrease is obtained to reveal a slow salinization of the pore fluid in this zone.

While electrical methods have been used for almost a century for oil and gas exploration in sand shale sequences, the electrical profiles might be used here to derive pore water electrical conductivity and, as a consequence, salinity for an equivalent pore fluid with  $\text{Na}^+$  and  $\text{Cl}^-$  ions only.

For this, a petrophysical calibration from cores and logs is needed from a detailed characterisation of the site, either in geological terms (depending upon the lateral variability of the site), or in hydrogeological (salinity of the pore fluid) and petrophysical (porosity, connectivity) terms.

The calibration corresponds to the subtraction from core and logs of the geologically invariant components of the signal. The data recorded by the observatory is therefore strongly influenced by site parameters with, in particular (i) the presence of clay, (ii) the porosity and (iii) pore fluid salinity.

### **Inversion of electrical resistivity in terms of NaCl equivalent pore fluid salinity**

From *Sundberg (1932)*, the electrical resistivity  $R_o$  of a porous media can be written as a simple product  $R_o = F.R_w$  of the electrical formation factor  $F$  by the resistivity  $R_w$  of the pore fluid (in  $\Omega.m$ ). After *Archie (1942)*, the electrical formation factor  $F$  is related to porosity by :

$$F = \emptyset^{-m} \quad (1)$$

with  $\emptyset$  for porosity and  $m$  as a connectivity term for porosity often called « cementation exponent » depending on pore shape, and varying from 1,3 for non consolidated sands to 2,5 for cemented carbonates, for example. Besides, a mean value of  $m = 2$  is often used in the absence of sufficient core measurements.

Since conductivity is the inverse of electrical resistivity, we have to the first order :

$$\frac{1}{R_o} = C_o = \frac{C_w}{F} \quad (2)$$

with  $C_o$  for porous media and  $C_w$  for pore fluid conductivity (both in mS/m).

When surface conduction cannot be neglected with respect to the volume, electrolytic term (in the presence of clays, for example), a more complete model is used (*Waxman et Smits, 1968*), integrating surface conductivity term ( $C_s$ ) with :

$$C_o = C_w / F + C_s \quad (3)$$

The surface conductivity term ( $C_s$ ) is related to the circulation of cations within the double layer in relation the cation exchange capacity (*CEC*) of the minerals. The *CEC* equates to the number of mobile cations in the pore space per unit mass, expressed in meq/100 g (ou en cmole/kg). Per unit volume, the *CEC* is called  $Q_v$  (expressed in eq/L equal to 96 320 C), with:

$$Q_v = \frac{(1 - \emptyset)}{\emptyset} \cdot \rho_m \cdot CEC \quad (4)$$

where  $\emptyset$  is porosity and  $\rho_m$  is grain density (in  $\text{kg/m}^3$ ). La conductivité électrique de surface du milieu s'écrit alors, toujours After *Revil et Glover (1998)*, the surface electrical conductivity is expressed in shaly sand by :

$$C_s = \frac{2}{3} \cdot \rho_m \cdot \beta_s \cdot CEC \quad (5)$$

where  $\beta_s$  accounts for cations mobility in the external part of the double layer. After *Revil et Glover, 1998*,  $\beta_s = 0,51 \cdot 10^{-8} \text{ m}^2 \cdot \text{s}^{-1} \cdot \text{V}^{-1}$  for a NaCl solution. The surface conductivity can therefore be measured for a series of core samples and compared to the potassium (K) content used here as an empirical proxy for clay content in the sediment. A linear regression relating surface conductivity to potassium content is obtained (*Figure 6*) :

$$C_s = (0.48) K - (31.7) \quad (6)$$

leading to the possibility to derive a continuous downhole log for the surface conductivity  $C_s$  from the potassium profile measured from spectral natural radioactivity. Once  $F$  computed on the basis of any porosity log such as that obtained from P wave velocities (*Wyllie et al., 1956*), the pore fluid conductivity  $C_w$  is directly obtained from :

$$C_w = (C_o - C_s) \cdot F \quad (7)$$



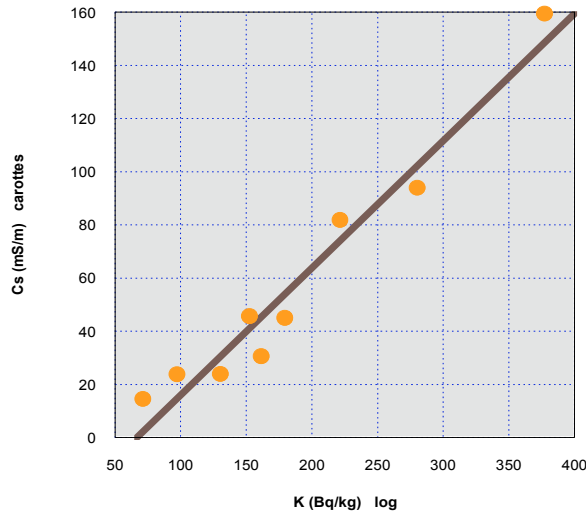


**Figure 6.** Surface electrical conductivity measured on core from MAG1 and plotted as a function of potassium content (K).

From Guéguen et Palciauska (1992), the pore fluid salinity is directly derived from :

$$\ln(s) = (0.97) \ln(C_w) - 4.88 \quad (8)$$

for a NaCl solution at 20°C. In the absence of values for the connectivity term  $m$ , two salinity profiles are presented for  $m=1.5$  and  $m=1.8$  (Figure 7). These two profiles almost overlap, underlining the low impact of  $m$  on the inversion. These inverted salinity profiles compare well with individual salinity values derived after chemical analysis in the laboratory from pore fluid samples obtained with the WestBay multi-packer completion (Table 1).

Port depth (m)	Ca (mg/l)	Mg (mg/l)	K (mg/l)	Na (mg/l)	Fe (mg/l)	Al (mg/l)	Cl (mg/l)	S (mg/l)	Si (mg/l)	Pore Fluid Salinity (g/l)
49.0	411.7	< 0.01	15.8	31.1	< 0.01	< 0.01	39.4	11.2	< 0.01	0.51
39.8	670.9	< 0.01	36.9	150.0	< 0.01	0.2	399.5	1.3	0.6	1.26
36.7	801.2	< 0.01	24.4	240.7	< 0.01	< 0.01	1108	3.5	0.7	2.18
32.1	387.7	< 0.01	17.4	514.8	< 0.01	< 0.01	1435	23.0	2.0	2.38
24.9	801.9	< 0.01	40.0	1282	< 0.01	< 0.01	3075	28.2	1.4	5.23
15.5	945.0	493.5	161.7	5342	< 0.01	< 0.01	12020	236.6	5.3	19.2
13.9	440.7	0.7	43.2	732.7	0.5	5.7	NA	46.5	13.7	NA
7.9	1023	< 0.01	110.6	2782	< 0.01	0.2	6195	101.9	1.7	10.2

**Table 1.** Pore fluid chemistry from fluid samples obtained in MAG5 with the WestBay multi-packer completion (June 2010). Very little amount of fluid was sampled from 13.9 m (with an alter impact on data quality in this case), while the other 7 intervals proved sufficient permeability for adequate sampling in a repeated manner.

In all, this inversion for MAG1 resistivity data at Maguelone points out the presence of sea water at 15 m depth in the aquifer, the inflow of fresh water from sands located at greater depth in the hole, and the overall diffusion process in clays throughout the sequence.

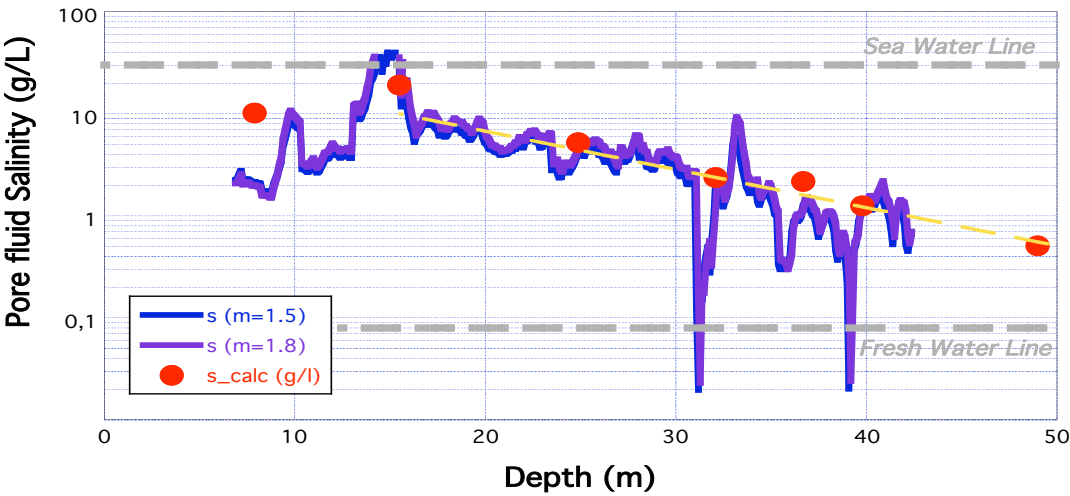


**Figure 7.** Pore fluid salinity profiles derived from downhole electrical resistivity data inverted after calibration from cores and logs, and compared to salinities directly measured from downhole fluid samples.

**Conclusion**

In summary, this new hydrogeophysical approach provides a high resolution means to follow at dm to meter scale the changes over time in pore fluid composition along a downhole section. This constitutes the basis to set-up a permanent monitoring strategy from in-situ, high frequency, autonomous observatories such as that of imaGeau.

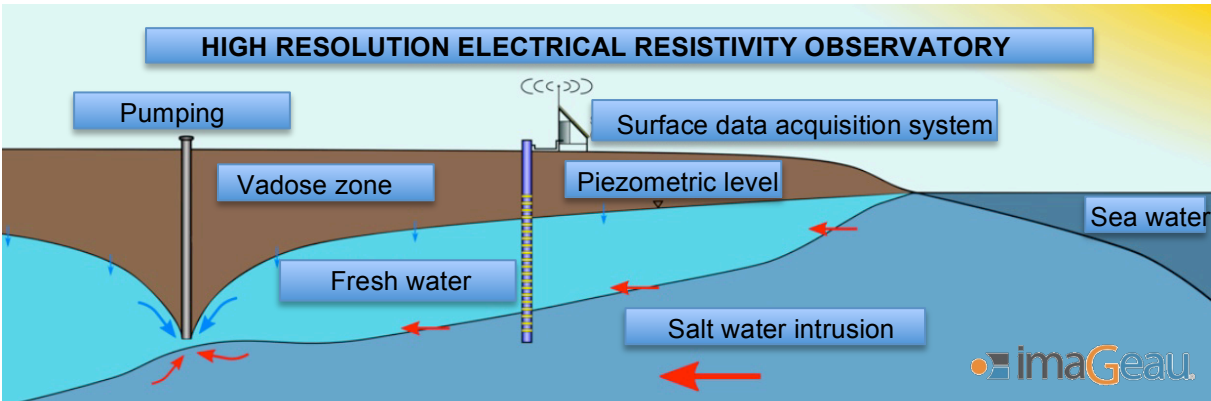


**Figure 8.** Salt-water intrusion high-frequency field monitoring set-up and principle from imaGeau downhole electrical resistivity observatory (sketch provided by imaGeau).

## References

- Archie, G.E. (1942). "The electrical resistivity log as an aid in determining some reservoir characteristics". *Petroleum Transactions of AIME* **146**: 54–62.
- Guéguen et Palciauska, 1992. Introduction à la physique des roches, p 192.
- Raynal, O., Bouchette, F., Certain, R., Séranne, M., Dezileau, L., Sabatier, P., Lofi, J., Bui Xuan Hy, A., Briquet, L., Pezard, P.A. and Tessier, B., 2009. Control of along shore-oriented sand spits on the dynamic of a wave-dominated coastal system (Holocene deposits, northern Gulf of Lions, France). *Marine Geology*, 264, 242-257.
- Revil A. et Cathles L.M., 1999, Permeability of shaly sands, *Water Resources Research* 35, 3, 651-662.
- Revil et Glover, 1998. Nature of surface electrical conductivity in natural sands, sandstones, and clays, *Geophysical Research Letters*, 25, 5, 691-694
- Waxman, M.H.; Smits, L.J.M. (1968). "Electrical conductivities in oil-bearing shaly sands". *SPE Journal* **8** (2): 107–122.
- Wyllie, M.R.J., Gregory, A. R., and Gardner, L. W., 1956. Elastic wave velocities in heterogeneous and porous media. *Geophysics*, 21, 41-70.